

PCA Benchmark Analysis with ADVANTG3.0.1. and MCNP6.1.1b Codes

Mario Matijević, Dubravko Pevec, Krešimir Trontl

University of Zagreb, Faculty of Electrical Engineering and Computing
Unska 3, 10000 Zagreb, Croatia

mario.matijevic@fer.hr, dubravko.pevec@fer.hr, kresimir.trontl@fer.hr

Bojan Petrović

Georgia Institute of Technology, Nuclear and Radiological Engineering
770 State St., Atlanta, GA 30332-0745, USA

bojan.petrovic@gatech.edu

ABSTRACT

The Pool Critical Assembly Pressure Vessel (PCA) benchmark is a well known benchmark in the reactor shielding community which is described in the Shielding Integral Benchmark Archive and Database (SINBAD). It is based on the experiments performed at the PCA facility in the Oak Ridge National Laboratory (ORNL) and it can be used for the qualification of the pressure vessel fluence calculational methodology. The measured quantities to be compared against the calculated values are the equivalent fission fluxes at several experimental access tubes (A1 to A8) in front, behind, and inside the pressure-vessel wall simulator. This benchmark is particularly suitable to test the capabilities of the shielding calculational methodology and cross-section libraries to predict in-vessel flux gradients because only a few approximations are necessary in the overall analysis. This benchmark was analyzed using a modern hybrid stochastic-deterministic shielding methodology with ADVANTG3.0.1 and MCNP6.1.1b codes. ADVANTG3.0.1 is an automated tool for generating variance reduction (VR) parameters for Monte Carlo (MC) calculations with MCNP5v1.60 code (and higher versions). It is based on the multigroup, discrete ordinates solver Denovo, used for approximating the forward-adjoint transport fluxes to construct VR parameters for the final MC simulation. The VR parameters in form of the weight windows and the source biasing cards can be directly used with unmodified MCNP input. The underlining CADIS methodology in Denovo code was initially developed for biasing local MC results, such as point detector or a limited region detector. The FW-CADIS extension was developed for biasing MC results globally over a mesh tallies or multiple point/region detectors. Both CADIS and FW-CADIS are based on the concept of the neutron importance function, which is a solution of the adjoint Boltzmann transport equation. The equivalent fission fluxes calculated with MCNP are based on several high-energy threshold reactions from international dosimetry libraries IRDF-2002 and IRDFF-2014, distributed by the IAEA Nuclear Data Section. The obtained results show a good agreement with referenced PCA measurements. Visualization of the deterministic solution in 3D was done using the VisIt code from the Lawrence Livermore National Laboratory (LLNL).

Keywords: *PCA benchmark, shielding, pressure vessel, Monte Carlo, variance reduction*

1 INTRODUCTION

Accurate knowledge of the reactor pressure vessel (RPV) irradiation with fast neutron fluence is one of the key safety requirements when determining the lifetime of a nuclear power plant. Another important aspect is the potential financial savings which could be achieved by approving nuclear power plant (NPP) lifetime extension. Modern calculational methods of reactor physics are successors of decades-long efforts to produce fast, reliable and predictive answers to challenging real-life problems, so any developed or analyzed calculation methodology requires comprehensive verification and validation against evaluated reference data. A large database of benchmarks aimed at validation of computer codes and nuclear data used for radiation transport and shielding problems is "Shielding Integral Benchmark Archive and Database (SINBAD)" [1]. One of the most widely used SINBAD benchmarks for qualification of radiation transport methods and evaluation of nuclear data for dosimetry calculations in Light Water Reactors (LWR) is the "Pool Critical Assembly Pressure Vessel Facility Benchmark" (PCA benchmark) [2].

The purpose of the PCA benchmark is to validate the capabilities of the computational shielding methodology to predict reaction rates in the regions outside of the reactor core when the neutron source, material compositions, and geometry are well defined. Over the years a number of PCA benchmark studies have been conducted using different calculational methods (discrete ordinates S_N method or Monte Carlo MC method) and dosimetry data libraries [3][4][5][6][7]. This paper presents another effort of the PCA benchmark analysis by using modern hybrid shielding methodology, where fast deterministic solution via discrete ordinates is used as a means to accelerate the final MC answer. Dosimetry cross-section data were extracted from the international library IRDF-2002 [8] for all dosimeters in order to be used as response functions. Such response functions have a meaning of the adjoint source spectrum which is an important physical parameter for variance reduction (VR) parameters construction. This paper is organized as follows. The PCA benchmark is described in Section 2. The description of the hybrid shielding methodology implemented in ADVANTG/MCNP codes is given in Section 3. The analysis of the PCA benchmark, including results of the criticality eigenvalue and fixed-source shielding calculations, is presented in Section 4. Conclusions are given in Section 5 while the referenced literature is given at the end of the paper.

2 PCA BENCHMARK FACILITY DESCRIPTION

The fast neutron fluence induced embrittlement of the reactor pressure vessel (RPV) is for some reactors the main cause for limiting the PWR power plant lifetime. With the advances of computer computational power the reactor dosimetry calculations can now give better insight into radiation damage of the RPV when exposed to intense neutron flux environment. For such purposes various correlations between neutron flux and irradiation effects of detectors have been established, such as displacement per atom (DPA), helium accumulation in reactor baffle plates by $^{58}\text{Ni}(n,\gamma)^{59}\text{Ni}(n,\alpha)^{56}\text{Fe}$ reaction sequence, etc. The current guideline for RPV dosimetry calculations is the U.S.NRC Regulatory Guide 1.190 [9], which states that calculational methods used to estimate RPV fast fluence should use the latest version of the Evaluated Nuclear Data File (ENDF/B) in the fast energy range (0.1–15) MeV. In accordance with this guideline, we present calculational results for the ORNL PCA Benchmark. The scope of PCA benchmark is to validate the capabilities of the calculational methodologies to predict the reaction rates in the region outside of the core when the neutron source, material compositions, and relatively simple geometry configuration are well defined and given. The PCA benchmark provides the calculated and measured reaction rates (C/M ratio) inside the simulated pressure vessel, as well as in the water gap in front of the pressure vessel. This allows an assessment of the accuracy with which the calculations predict the neutron flux attenuation inside the pressure vessel. The PCA benchmark

facility consists of the reactor core and the components that mock up the reactor-to-cavity region in typical light water reactors. These components are the thermal shield (TS), the reactor pressure vessel simulator (RPVS), and the void box (VB), which simulates the reactor cavity. The Monte Carlo simulation model of the PCA benchmark facility is shown in Figure 1.

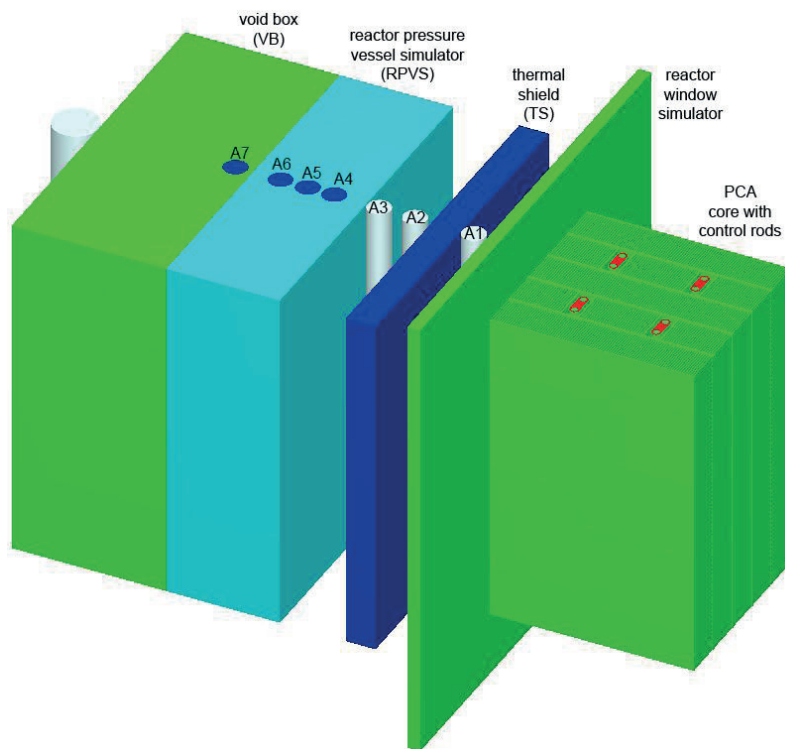


Figure 1: MC model of the PCA benchmark facility (water removed)

The large aluminum plate in front of the PCA core, referred to in Figure 1 as the reactor window simulator, was added to the facility for operational reasons. The thicknesses of the water gaps between the aluminum window and thermal shield and between the thermal shield and pressure vessel are approximately 12 cm and 13 cm, respectively. Such PCA configuration is known as "12/13" configuration. The materials used for the components outside the core were aluminum for the reactor window simulator, stainless steel for the thermal shield, and carbon steel for the pressure vessel. The PCA facility is located in a large pool of water (removed in Figure 1), which serves as reactor core coolant and moderator and provides extra shielding. The PCA benchmark facility core is a light water moderated, highly enriched uranium ($e=93\%$) fueled critical assembly. It consists of 25 material test reactor (MTR) plate type elements. The standard MTR fuel element and control element are depicted in Figure 2.

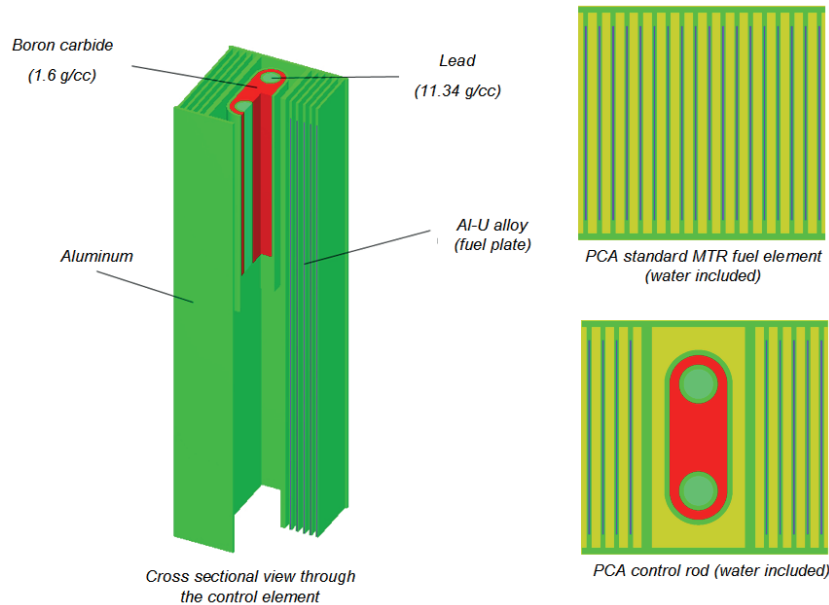


Figure 2: Standard MTR and control element of the PCA core

The eight vertical experimental access tubes (A1-A8) in which the measurements were done were filled with appropriate material (steel in the pressure vessel locations and Plexiglas in the in-water locations) in order to minimize the perturbations of the neutron field. Measured quantities, used in the PCA benchmark, are given in terms of the equivalent ^{235}U fission fluxes which were calculated by dividing the reaction rates with the cross-sections averaged over the ^{235}U fission spectrum [2]. All measured quantities provided for comparison with calculated DORT values are given per unit PCA benchmark facility core neutron source, meaning that they are normalized to a unit source. Therefore, the calculated results need to be normalized to the source strength of one fission neutron per second being born in the whole PCA core. The ratios of the calculated-to-measured (C/M) equivalent fission fluxes for DORT libraries BUGLE-93, SAILOR-95, and BUGLE-96 are given in PCA benchmark reference [2]. Measurements were performed at the core midplane ($z = 0$) at several locations, labeled in Figure 3 as A1 to A7.

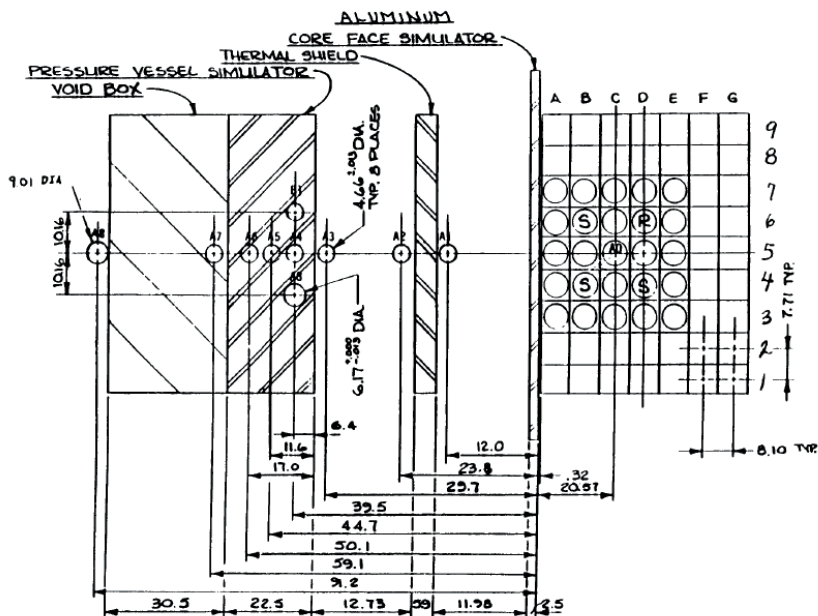


Figure 3: Horizontal cross section of the PCA pressure vessel benchmark facility "12/13" [2]

To complete the PCA benchmark analysis the analyst must determine the calculated-to-measured (C/M) ratios of the equivalent ^{235}U fission fluxes for all the locations and all the dosimeters for which the measured values are provided. The significance of the PCA Benchmark are the *experimental data measurements* inside the thick steel RPV in locations A4 to A6, that is, the neutron flux gradient inside the pressure vessel, which provides the means for verification of calculated neutron flux attenuation. This is in contrast to available data from existing operating reactors, which are typically addressing neutron flux for downcomer region internal to RPV and reactor cavity external to RPV wall [10].

3 HYBRID SHIELDING METHODOLOGY WITH ADVANTG/MCNP

The ADVANTG3.0.1 [11] is an automated tool for generating variance reduction parameters for fixed-source continuous-energy MC simulations with MCNP6.1.1b code [12], based on approximate 3D multigroup discrete ordinates forward-adjoint transport solutions generated by Denovo [13]. The Denovo is a structured, Cartesian grid S_N solver based on the Koch-Baker-Alcouffe parallel transport sweep algorithm across the x-y domain blocks. Denovo is used in forward and adjoint mode to approximate the space-energy dependent flux across the S_N mesh. These solutions are utilized to calculate space-energy dependent biasing parameters, biased source and transport importance map (weight windows), to be used as VR parameters in the MCNP. CADIS methodology [14] is used to optimize MC results in localized regions of phase-space, while FW-CADIS [15] is applied to obtain global uniform statistical uncertainty by weighting the adjoint source with expected detector response approximated with forward Denovo solution. CADIS and FW-CADIS are based on the adjoint function [16] (i.e., solution of the adjoint Boltzmann equation) which has long been recognized as the importance function for some objective function of interest. Detector response is found by integrating the product of the detector cross-section $\sigma_d(\vec{r}, E)$ and flux over detector volume:

$$R = \int_{V_D} \int_E \sigma_d(\vec{r}, E) \phi(\vec{r}, E) dV dE \quad (1)$$

Alternatively, if we approximate the adjoint scalar flux with a quick Denovo solution, where the adjoint source is set as $q^\dagger(\vec{r}, E) = \sigma_d(\vec{r}, E)$, then the detector response is found by integrating the product of the normal source distribution q and the adjoint flux over the source volume:

$$R = \int_{V_S} \int_E q(\vec{r}, E) \phi^\dagger(\vec{r}, E) dV dE . \quad (2)$$

The biased source distribution $\hat{q}(\vec{r}, E)$ [11], which minimizes the variance of a user-desired response R , can be found by using the Lagrange multiplier λ method [17],

$$L[\hat{q}(\vec{r}, E)] = \int_V \int_E \frac{q^2(\vec{r}, E) (\phi^\dagger(\vec{r}, E))^2}{\hat{q}(\vec{r}, E)} dV dE + \lambda \int_V \int_E \hat{q}(\vec{r}, E) dV dE , \quad (3)$$

giving the final expression for a biased source

$$\hat{q}(\vec{r}, E) = \frac{\phi^\dagger(\vec{r}, E) q(\vec{r}, E)}{R} = \frac{\phi^\dagger(\vec{r}, E) q(\vec{r}, E)}{\int_{V_S} \int_E q(\vec{r}, E) \phi^\dagger(\vec{r}, E) dV dE} , \quad (4)$$

where $\phi^\dagger(\vec{r}, E)$, $q(\vec{r}, E)$ and R are the scalar adjoint function, the source emission probability (forward source), and the total detector response, respectively. For transport biasing the weight window technique is employed, that is, space-energy dependent geometric splitting/roulette. Biased source and weight-window lower bounds are consistent, so the source particles are created with statistical weights within weight windows:

$$\bar{w}(\vec{r}, E) = \frac{q(\vec{r}, E)}{\hat{q}(\vec{r}, E)} = \frac{R}{\phi^\dagger(\vec{r}, E)} = \frac{\int_{V_s} \int_E q(\vec{r}, E) \phi^\dagger(\vec{r}, E) dV dE}{\phi^\dagger(\vec{r}, E)}. \quad (5)$$

Inverse relationship between the particle statistical weight and adjoint function must be emphasized. Since the PCA Benchmark involves calculation of near and far detector reaction rates, this FW-CADIS methodology was a highly desirable choice. The VR parameters generated by ADVANTG consist of space-energy dependent weight-window bounds (WWINP file) and biased source distributions (SB cards in SDEF), which are outputted in formats that can be directly used with unmodified version of MCNP. ADVANTG has been applied to neutron, photon, and coupled neutron-photon simulations of real-world radiation detection and shielding scenarios. ADVANTG is compatible with all MCNP geometry features and can be used to accelerate cell tallies (F4, F6, F8), surface tallies (F1 and F2), point-detector tallies (F5), and Cartesian mesh tallies (FMESH).

The MCNP6.1.1b is a general-purpose Monte Carlo N-Particle code that can be used for neutron, photon, electron, or coupled neutron/photon/electron transport. The MCNP treats an arbitrary three-dimensional configuration of materials in geometric cells bounded by first- and second-degree surfaces and fourth-degree elliptical tori. For neutrons, all reactions given in a particular cross-section evaluation (such as ENDF/B-VI) are accounted for. Thermal neutrons are described by both the free gas and $S(\alpha, \beta)$ models. Important standard features that make MCNP very versatile and easy to use include a powerful general source, criticality source, and surface source; both geometry and output tally plotters; a rich collection of variance reduction techniques; a flexible tally structure; and an extensive collection of cross-section data. Energy ranges are from 1e-11 to 20 MeV for neutrons with data up to 150 MeV for some nuclides, 1 keV to 1 GeV for electrons, and 1 keV to 100 GeV for photons. Pointwise cross-section data were used within MCNP: auxiliary program MAKXSf prepares cross-section libraries with Doppler broadening.

4 ANALYSIS OF THE PCA BENCHMARK

The Monte Carlo calculational model of the PCA facility was developed using combinatorial geometry of the MCNP code. The model was verified with criticality eigenvalue calculation while the obtained equivalent fission fluxes have been compared with the referenced PCA benchmark data.

4.1 Criticality eigenvalue results

The criticality eigenvalue calculation of the PCA benchmark facility was performed using 350 active neutron cycles with 2000 neutrons per cycle. First 50 cycles were skipped in order for the fission source distribution to converge to the fundamental eigenmode, which was confirmed with the Shannon entropy check. Geometry of the system, materials, and critical control rod positions were verified yielding the effective neutron multiplication factor of the system $k_{\text{eff}} = (0.99924 \pm 0.00100)$.

4.2 Fixed source shielding results

The FW-CADIS methodology of the ADVANTG code was used for the VR preparation in form of the consistent weight windows and biased source distributions for biasing neutron transport from the PCA core to eight detector locations in the experimental access tubes A1–A8. The equivalent fission fluxes in the PCA report were calculated by dividing the reaction rates by the cross-sections averaged over the ^{235}U fission spectrum. Equivalent fission fluxes are thus defined as

$$\phi_{eq} = \frac{\int_E \sigma_i(E)\phi(E)dE}{\int_E \sigma_i(E)\varphi(E)dE} = \frac{\text{reaction rates}}{\bar{\sigma}_i} \quad (6)$$

where $\sigma_i(E)$, $\phi(E)$ and $\varphi(E)$ are dosimetry cross-sections for the reaction of interest, the Monte Carlo flux at the dosimetry location (center of experimental tubes), and weighting spectrum function, respectively. The spectrum-averaged cross-sections $\bar{\sigma}_i$ were taken from the referenced PCA benchmark Table 1.6 [2] for the sake of consistency, but they were independently cross-checked with our libraries. Seven point detector locations (A1 to A7) were tallied for total of six reaction rates of interest using IRDF-2002 library: $^{237}\text{Np}(n,f)^{137}\text{Cs}$, $^{238}\text{U}(n,f)^{137}\text{Cs}$, $^{103}\text{Rh}(n,n')^{103m}\text{Rh}$, $^{115}\text{In}(n,n')^{115m}\text{In}$, $^{58}\text{Ni}(n,p)^{58}\text{Co}$, and $^{27}\text{Al}(n,\alpha)^{24}\text{Na}$. These reactions were used as response functions for the FW-CADIS methodology, corresponding to point adjoint source spectrum. The threshold energies for the $^{27}\text{Al}(n,\alpha)^{24}\text{Na}$, $^{58}\text{Ni}(n,p)^{58}\text{Co}$, $^{238}\text{U}(n,f)^{137}\text{Cs}$, $^{237}\text{Np}(n,f)^{137}\text{Cs}$, $^{115}\text{In}(n,n')^{115m}\text{In}$, and $^{103}\text{Rh}(n,n')^{103m}\text{Rh}$ reactions are 5.0, 2.05, 1.45, 0.69, 0.3, and 0.1 MeV, respectively. Even though majority of the reactions are in the fast neutron range, MCNP calculations were performed with full neutron spectrum using continuous energies.

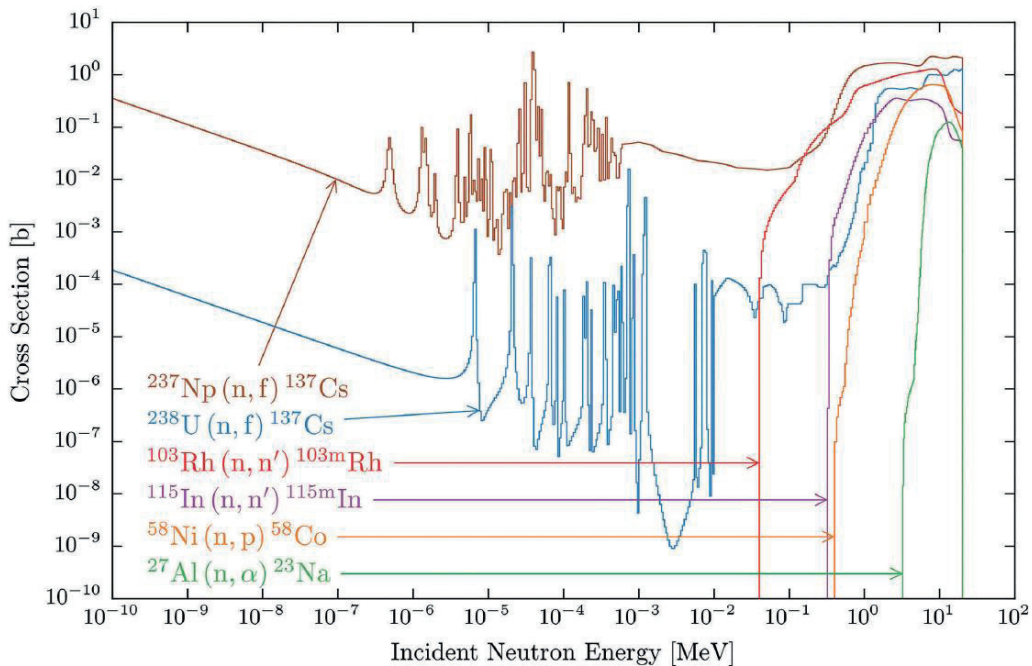


Figure 4: Reaction cross sections of interest in the PCA benchmark

The ADVANTG code with FW-CADIS methodology was used with updated "bplus" ANISN-type multigroup shielding library (47n/20g), containing 393 isotopes and based on the ENDF/B-VII.0 nuclear data [18][19]. The robust and flux-positive step characteristic (SC) spatial differencing scheme was used in S_N calculations. The "macromaterial" option was used to mix 11 pure materials

into 26857 effective Denovo materials. Point detectors were placed in the center of void spheres which are located in the axial midplane of the experimental tubes. The Denovo S_N mesh had 1.6×10^6 cells covering the PCA facility model, that is, $160 \times 100 \times 100$ cells in the xyz direction with average cell side of 1.0 cm. The same mesh size was used for the MCNP mesh tally. The quadrature set was quadruple QR (2 polar x 2 azimuth per octant) and Legendre order of scattering cross-section expansion was P_1 (upscattering was deactivated). Since the axial flux gradients inside tubes are confirmed to be sufficiently small, void spheres with 1.0 cm radius were also placed in the midplane ($z = 0$) of the access tubes, to verify point detector results. The ADVANTG memory consumption is highly dependent on the adjoint source spectrum function, so the forward run used 6-9 GB RAM and adjoint run used 10-14 GB RAM. The MCNP was run for 3 hrs in parallel mode utilizing PVM routine with 4 CPU cores which resulted in 2-4 million histories. Point detectors had on the average less than 1% statistical relative error (RE). Selected ADVANTG and MCNP results for $^{27}\text{Al}(n,\alpha)^{24}\text{Na}$ reaction are presented next. Figure 5 shows Denovo fast (7.4 – 6.1 MeV) and thermal (1e-05 – 0.1 eV) neutron flux solutions, with characteristic gradients in thick steel regions. Figure 6 shows Denovo total (integrated) adjoint flux where local maxima correspond to point detector locations. The most distant detector A8 has the highest peak, since the probability of neutron transport to that location is extremely low.

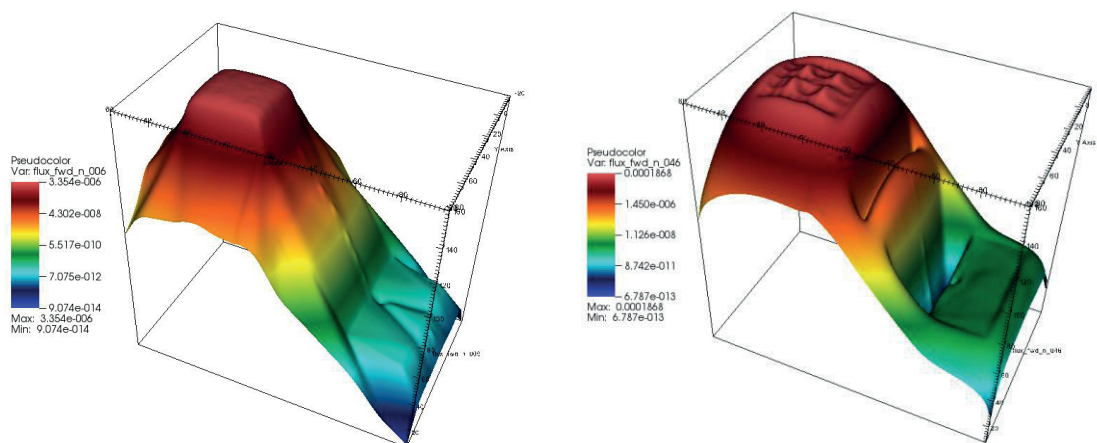


Figure 5: Denovo neutron flux solution in the PCA midplane (left: fast group no. 6; right: thermal group no. 46)

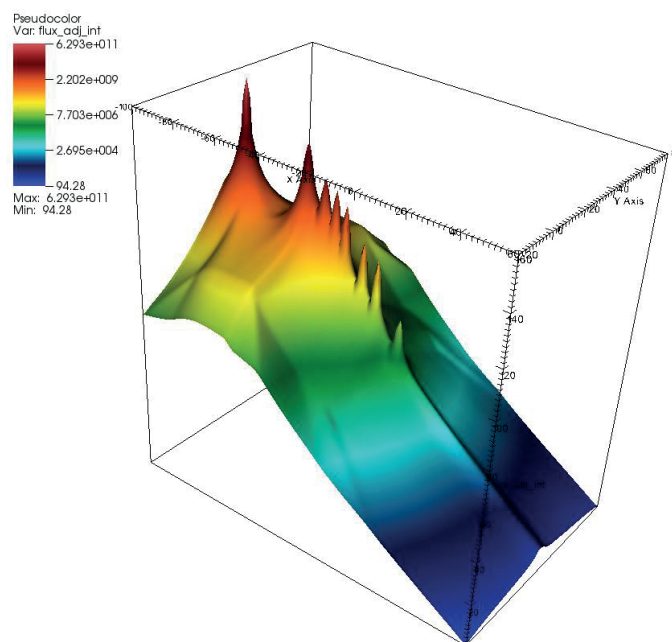


Figure 6: Denovo integrated total adjoint flux in the PCA midplane

The weight windows for the first energy group (17.3 – 14.2 MeV) are shown in Figure 7, where one can notice the expected $\bar{w}(\vec{r}, E) = R / \phi^\dagger(\vec{r}, E)$ behavior. Figure 8 and Figure 9 are depicting MCNP mesh tally solution in the PCA midplane with relative errors. One can notice that regions with smallest statistical error correspond to point detector locations.

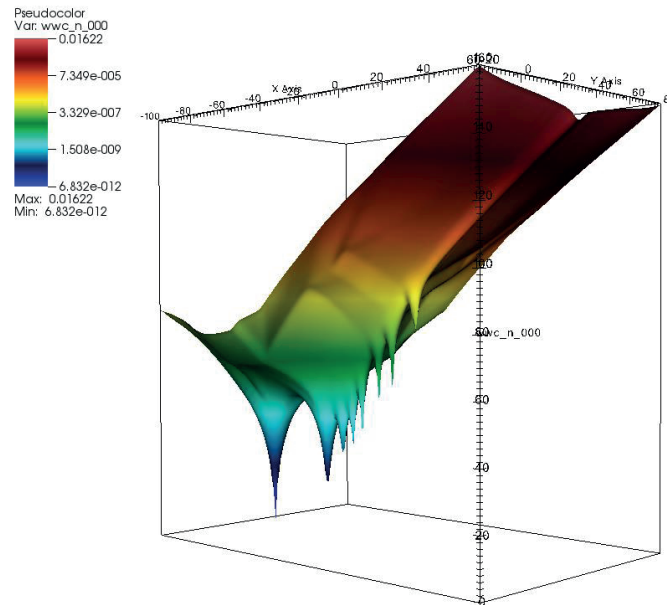


Figure 7: Denovo weight windows in the PCA midplane (fast group no. 1)

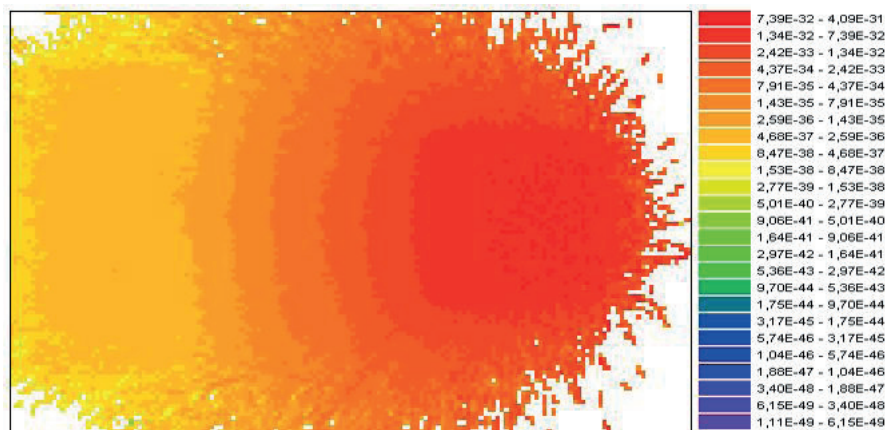


Figure 8: MCNP $^{27}\text{Al}(n,\alpha)^{24}\text{Na}$ reaction rates in the PCA midplane

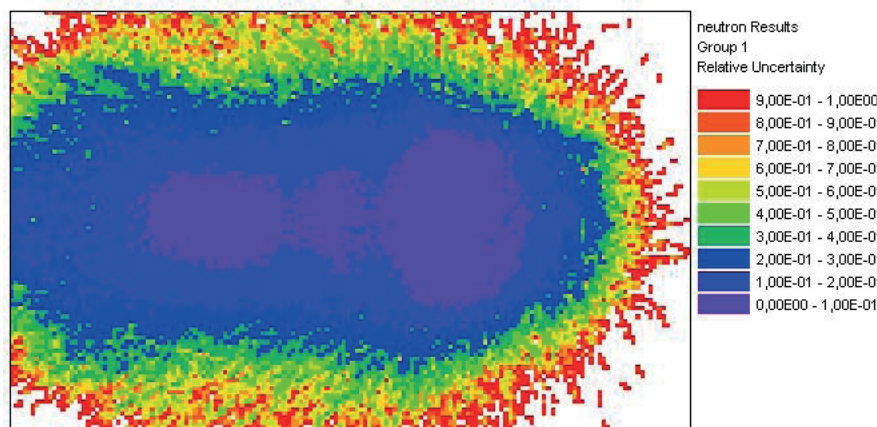


Figure 9: MCNP relative error of $^{27}\text{Al}(n,\alpha)^{24}\text{Na}$ reaction rates in the PCA midplane

The MCNP calculated equivalent fission fluxes C/M ratios are shown in Table 1. Average C/M per location is also shown with one standard deviation. Only the reactions for which the PCA measurements were reported are listed. These results are compared to the referenced DORT results [2], where one can notice high similarity between the stochastic and deterministic solution methods. Locations A4 to A6 highlighted in yellow are for the detectors placed inside the RPV simulator.

Table 1: Equivalent fission fluxes C/M ratios*

Location	$^{237}\text{Np}(n,f)$	$^{238}\text{U}(n,f)$	$^{27}\text{Al}(n,\alpha)$	$^{58}\text{Ni}(n,p)$	$^{115}\text{In}(n,n')$	$^{103}\text{Rh}(n,n')$	MCNP Avg \pm sig	DORT Avg \pm sig
A1	0.86	-	0.85	0.99	1.01	1.01	0.94 ± 0.04	0.91 ± 0.02
A2	-	-	0.91	1.05	1.10	-	1.02 ± 0.06	0.92 ± 0.01
A3	0.91	-	0.80	0.90	0.93	-	0.89 ± 0.03	0.96 ± 0.02
A4	0.87	0.88	0.90	0.98	0.97	0.94	0.92 ± 0.02	0.94 ± 0.03
A5	0.91	0.88	0.96	1.02	0.99	0.95	0.95 ± 0.02	0.92 ± 0.03
A6	0.88	0.88	1.01	1.04	1.02	0.96	0.97 ± 0.03	0.91 ± 0.04
A7	0.94	-	-	-	-	-	0.94 ± 0.00	0.89 ± 0.00
A8	-	-	-	-	-	-	-	-

(*"- experimental results were not provided in the PCA benchmark)

5 DISCUSSION OF RESULTS

The obtained MCNP results for the equivalent fission fluxes are in accordance with the calculational uncertainty criterion from the U.S.NRC Regulatory Guide 1.190, meaning that the calculated values agree with the measurements to within 20% for out-of-core dosimetry locations. Underprediction in the C/M ratio can be observed for the reaction $^{238}\text{U}(n,f)^{137}\text{Cs}$ (1.45 MeV threshold) through the thick RPV simulator (locations A4 to A6), with 0.88 on average. High attenuation of the neutron flux in that area is causing softening of the neutron spectrum in the RPV simulator, which shifts neutrons in resonance regions for inelastic scattering on iron isotopes. Microscopic cross-section for neutron inelastic scattering on iron isotopes is shown in Figure 10 [20][21].

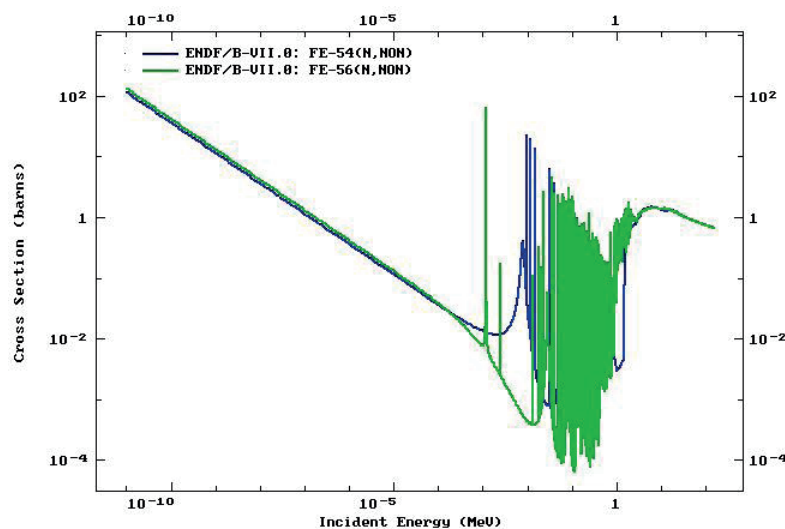


Figure 10: Inelastic scattering (MT=3) of iron isotopes

Results for $^{238}\text{U}(n,f)^{137}\text{Cs}$ can indicate self-shielding effects and sensitivity of the multigroup shielding library "bplus" on the iron cross sections. Overprediction in results is highest for the

detector A2 with average C/M ratio of 1.02, immediately after the stainless steel thermal shield, which has large amount of iron. Again, self-shielding effects of iron cross-sections are pronounced, especially for $^{27}\text{Al}(n,\alpha)^{24}\text{Na}$ with C/M ratio of 0.91. The obtained MCNP results show an overall good agreement with the experimental results, however, for location A3 in front of the RPV simulator there is underprediction about 10% on average.

Another indicator of an efficient hybrid shielding MC simulation is the adjusted figure-of-merit (FOM) factor [11][12]. It is introduced to account for the time it takes to achieve a given level of uncertainty in a MC simulation

$$FOM = 1 / RE^2 (T_{MC} + T_{ADV}), \quad (7)$$

where RE is the tally relative error (on 1 sigma level), T_{MC} is the MCNP run time (in min), and T_{ADV} is the ADVANTG run time (in min). This adjusted FOM factor can be used to determine whether ADVANTG-based VR parameters are worth the time that was required to generate them. This useful metric was a bit abused in this paper by making T_{MC} larger than what is actually required in practical application. This is evident since the average point detector RE is below 1 %, while an acceptable value by the MCNP manual is 5% or less. General trend of decreasing FOM factors on Figure 11 towards distant detectors means that it is a hard task to transport neutrons through thick layers of water and steel, so more histories (i.e. CPU time) is necessary to achieve the same level of uncertainty. In this paper all calculations have been performed on QuadCore Q6600 with 8GB of RAM.

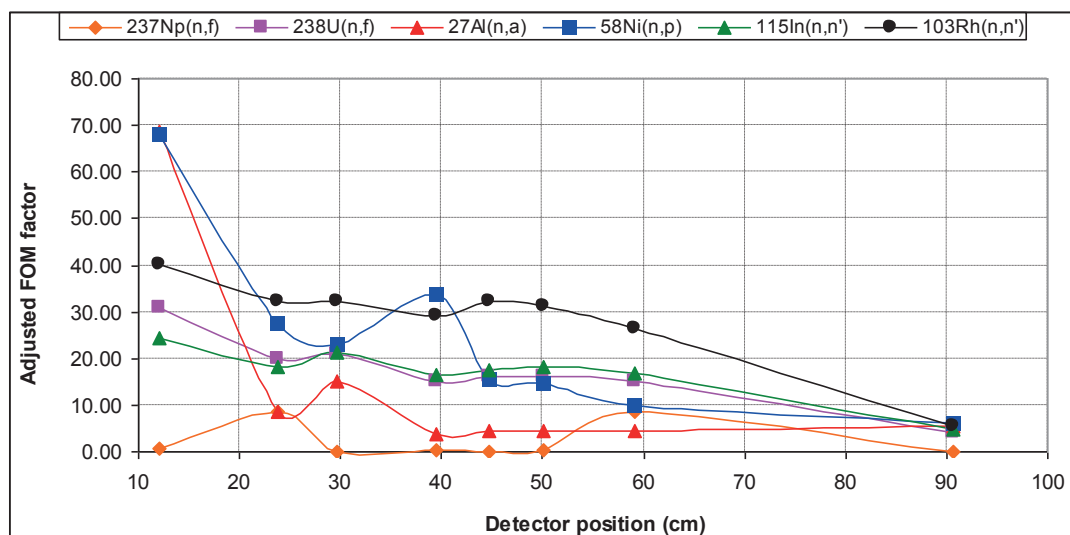


Figure 11: MCNP adjusted FOM factors for different detector locations

6 CONCLUSIONS

The simulation model of the PCA benchmark facility was developed using MCNP and ADVANTG codes, implementing modern hybrid shielding techniques. The results of shielding calculations in form of equivalent fission fluxes have been compared with PCA reference data. A good agreement of the calculated and measured equivalent fission fluxes has been obtained. No systematic decrease of agreements between calculations and measurements with increasing distance of detector from the PCA core was observed. This indicates that the shapes of calculated neutron spectra, in the energy range where dosimeters are sensitive, are properly determined. Application of the automated variance reduction technique based on FW-CADIS methodology removes the burden of manually tuning the VR parameters and significantly improves the quality of MC calculations.

REFERENCES

- [1] "Shielding Integral Benchmark Archive and Database," SINBAD Reactor Shielding Benchmark Experiments, OECD/NEA, 2011.
- [2] I. Remec and F. B. Kam, "Pool Critical Assembly Pressure Vessel Facility Benchmark," NUREG/CR-6454 (ORNL/TM-13205), prepared for the U.S.NRC by Oak Ridge National Laboratory, August 1997.
- [3] A.H. Fero, S.L. Anderson, and G.K. Roberts, "Analysis of the ORNL PCA benchmark using TORT and BUGLE-96," in *Reactor Dosimetry: Radiation Metrology and Assessment*, J.G. Williams, D. W. Vehar, F. H. Ruddy, and D. M. Gilliam, Eds., pp. 360–366, American Society for Testing and Materials, Philadelphia, Pa, USA, 2001.
- [4] Y.K. Lee, "Analysis of the NRC PCA pressure vessel dosimetry benchmark using TRIPOLI-4.3 Monte Carlo code and ENDF/BVI.4, JEF2.2 and IRDF-90 libraries," *Nuclear Mathematical and Computational Science: A Century in Review, A Century A new*, Gatlinburg, Tenn, USA, April 2003.
- [5] T. Flaspöehler, B. Petrovic, "Validating SCALE6.1/MAVRIC with Two Reactor Pressure Vessel Dosimetry Benchmarks," *Trans. Am. Nucl. Soc.*, 106, (2012).
- [6] M. Matijević, D. Pevec, K. Trontl, "Modeling of the ORNL PCA Benchmark Using SCALE6.0 Hybrid Deterministic-Stochastic Methodology," *Science and Technology of Nuclear Installations*, Vol. 2013, Article ID 252140, 2013.
- [7] J.A. Kulesza and R.L. Martz, "Evaluation of the Pool Critical Assembly Benchmark with Explicitly Modeled Geometry Using MCNP6," *Nuclear Technology* 197:3, 284-295, 2017.
- [8] International Atomic Energy Agency, Vienna, Austria, "International Reactor Dosimetry File 2002 (IRDF-2002)," 2006.
- [9] U.S.NRC, "Calculational and Dosimetry Methods for Determining Pressure Vessel Neutron Fluence," *Regulatory Guide 1.190*, 2001.
- [10] I. Remec and F. B. K. Kam, "H.B. Robinson-2 Pressure Vessel Benchmark," NUREG/CR-6453 (ORNL/TM-13204), prepared for the U.S.NRC by Oak Ridge National Laboratory, October 1997.
- [11] S.W. Mosher, S.R. Johnson, A.M. Bevil et al., "ADVANTG – An Automated Variance Reduction Parameter Generator," ORNL/TM-2013/416, Rev. 1, August 2015.
- [12] T. Goorley, "MCNP6.1.1-Beta Release Notes," LA-UR-14-24680, 2014.
- [13] T.M. Evans, A.S. Stafford, R.N. Slaybaugh, K.T. Clarno, "Denovo: A New Three-Dimensional Parallel Discrete Ordinates Code in SCALE," *Nuclear Technology*, 171:2, 171-200, DOI: 10.13182/NT171-171, 2010.
- [14] J.C. Wagner and A. Haghghat, "Automated variance reduction of Monte Carlo shielding calculations using the discrete ordinates adjoint function," *Nuclear Science and Engineering*, Vol. 128, no. 2, pp. 186–208, 1998.

- [15] J.C. Wagner, E. D. Blakeman, and D. E. Peplow, "Forward weighted CADIS method for global variance reduction," Transactions of the American Nuclear Society, vol. 97, pp. 630–633, 2007.
- [16] G.I. Bell and S. Glasstone, "Nuclear Reactor Theory," Van Nostrand Reinhold Company, Litton Educational Publishing, 1970.
- [17] D.H. Kim, et al, "A proposal on multi-response CADIS method to optimize reduction of regional variances in hybrid Monte Carlo simulation," Annals of Nuclear Energy 104, 282-290, 2017.
- [18] J.M. Risner, D.Wiarda, M.E. Dunn, T.M. Miller, D.E. Peplow, and B.W. Patton, "Production and Testing of the VITAMIN-B7 Fine-Group and BUGLE-B7 Broad-Group Coupled Neutron/Gamma Cross-Section Libraries Derived from ENDF/B-VII. 0 Nuclear Data," U.S.NRC NUREG/CR-7045, 2011.
- [19] M.B. Chadwick, P. Obložinsky, M. Herman et al., "ENDF/B-VII.0: next generation evaluated nuclear data library for nuclear science and technology," Nuclear Data Sheets, Vol. 107, no. 12, pp. 2931–3060, 2006.
- [20] A. Trkov, M. Herman, and D. A. Brown, "ENDF-6 Formats Manual," Data Formats and Procedures for the Evaluated Nuclear Data Files ENDF/B-VI and ENDF/B-VII, National Nuclear Data Center, Brookhaven National Laboratory, 2011.
- [21] IAEA Nuclear Data Services, <http://www-nds.iaea.org/>, last accessed on May 2018.